ELSEVIER

Biophysical Chemistry 80 (1999) 119–128

Biophysical Chemistry

www.elsevier.nl/locate/bpc

A statistical mechanical theory for the adsorption of protein to liposomal membranes

Y. Suezaki[a,*], H. Ichinose[a], K. Takiguchi[b], H. Hotani[b]

[a] *Department of General Education, Physics Laboratory, Saga Medical School, Saga 849-8501, Japan*
[b] *Division of Molecular Biology, Graduate School of Science, Nagoya University, Nagoya 46401, Japan*

Received 4 March 1999; received in revised form 7 May 1999; accepted 7 May 1999

Abstract

The observed topology change of spherical lipid vesicles to coffee cups [Saitoh, A. et al., Proc. Natl. Acad. Sci. USA 95 (1998) 1026] was analyzed by a statistical mechanical theory. The topology change was due to the adsorption of talin molecules to the orifices of the coffee cups. The adsorption isotherm of talin between an aqueous solution and the vesicle membrane was analyzed by taking account of the bending energy of the membrane. The equilibrium is determined by the balance of the energy gain for the adsorption of talin to the periphery of the vesicles and the change of the bending energy of the membrane due to the shape change. The observed coexistence of coffee cups and sheet-like vesicles were reproduced. Vesicles with two orifices were also analyzed and theoretically reproduced.

Keywords: Lipid membrane; Adsorption of protein; Bending modulus; Statistical mechanics

---

1. Introduction

Lipid bilayer membranes form various morphologies such as spherical vesicles, tubules and lamellar structures in aqueous solution depending on the materials, preparations, boundary conditions, and other factors. By combining with other molecules, the variety of morphologies of lipid membranes can be expanded further. Our group also observed several interesting phenomena in the systems of lipid membranes and proteins [1,2].

Recently, Saitoh et al. [3] observed a dramatic shape change of spherical lipid vesicles to coffee cup shaped vesicles, vesicles with more than a single orifice, and sheet-like vesicles by adding

---

[*] Corresponding author. Tel.: +81-952-34-2194; fax: +81-952-34-2022.
E-mail address: suezaki@post.saga-med.ac.jp (Y. Suezaki)

PII: S0301-4622(99)00065-4

talin (cytoskeletal submembranous protein) to aqueous solvents. The adsorption of talin to the peripheries of the coffee cups, sheets, etc., was confirmed by dark-field microscope and fluorescence methods. With concentrations of $> 1\ \mu M$ talin, coffee cup shaped vesicles appeared, which coexisted with the spherical vesicles. By increasing the concentration further, sheet-like vesicles appeared and coexisted with the coffee cups. The fraction of the sheets increased with additional talin [3].

To explain the above interesting phenomena, we formulated a statistical mechanical formula for the adsorption of talin to the vesicles. De-

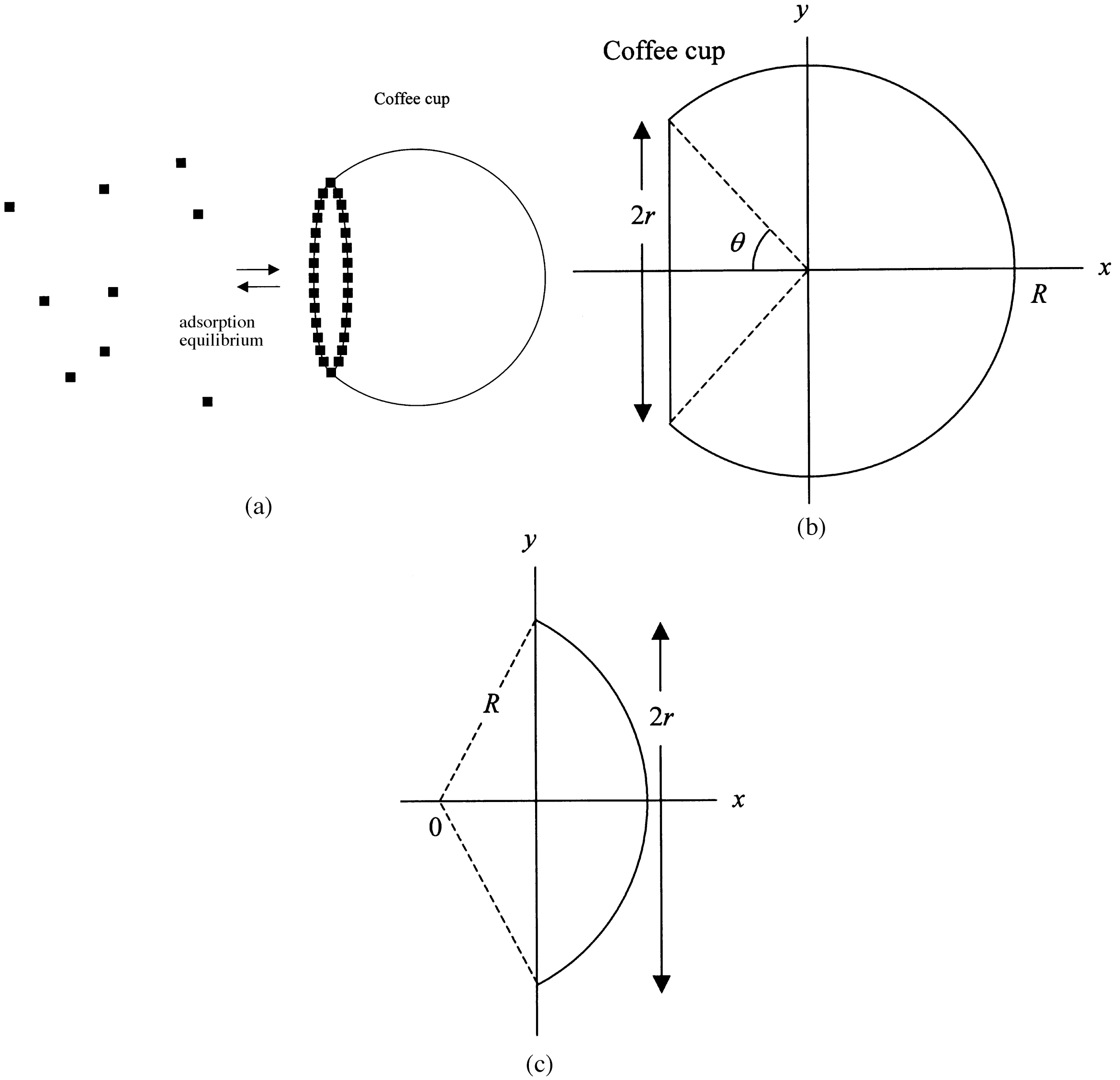

Fig. 1. Schematic picture of adsorbed talin to the vesicle and geometrical pictures of the coffee cups: (a) schematic picture of adsorbed talin to the vesicle; (b) geometrical showing of the coffee cup with a small orifice; (c) geometrical showing of the coffee cup with a large orifice.

pending on the experimental procedure, the initial spherical vesicles made in the laboratory [3] may not be in true equilibrium but might be in a metastable state. For several tens of minutes that are shorter than the lifetime of the vesicles, however, we can assume the metastable state as a starting point. The talin molecule is adsorbed at the orifice of the vesicle due to the hydrophobic nature of the part of the talin molecule. Fig. 1a shows a schematic drawing of the adsorption of talin to the vesicle.

We employ the bending energy of membranes as the energy of shape change of the vesicles. The general form of the bending energy is written as

$$E_{\text{bend}} = \frac{\kappa}{2}\int\int (c_x + c_y - c_0)^2 \mathrm{d}S \tag{1}$$

where κ, c_x, c_y, and c_0 are the bending modulus of the membrane, two principal curvatures and the spontaneous curvature, respectively [4]. The integral is taken over the surface of the membrane. Eq. (1) has been employed by many workers as a model of mechanical membrane energy [5,6]. We do not take account of the Gaussian curvature term. It is because the appearance of the periphery in the shape change from the spherical vesicle to the coffee cup vesicle does not cost the bending energy.

The spontaneous curvature of the bilayer membrane is usually assumed to be zero. However, this idea is based on the assumption that the membrane system is in equilibrium. As we stated before, the vesicles were not necessarily in the equilibrium state but were made by mechanical agitation or were under some specific boundary conditions of the system [3]. As the turn-over time of a lipid molecule from one monolayer to the other is very long, artificially made vesicles could initially possess non-zero spontaneous curvatures [7–9].

The adsorption of talin to the periphery of the vesicles is formulated in detail in Section 2. In Section 3, a semi-quantitative evaluation of the theory and the observed data is made. Also, vesicles with other shapes are analyzed. In Section 4, conclusion and discussion will be given.

2. Theoretical formulation

First, the bending energy of a coffee cup shaped vesicle is calculated. Fig. 1b shows the geometrical definition of the coffee cup. The initial radius of the spherical vesicle is defined as R_0. The radii of the coffee cup and its orifice are denoted as R and r, respectively. The actual shape of the cup is a little different from ours [3], but we employ the shape given in Fig. 1b as a first approximation. Because the surface area of the vesicle is conserved upon deformation, the surface area, S, is given as

$$S = 2\pi R^2\left(1 + \sqrt{1 - \left(\frac{r}{R}\right)^2}\right) \tag{2}$$

which is identical to the surface area of the sphere

$$S = 4\pi R_0^2 \tag{3}$$

When a vesicle deforms further, the shape becomes that shown in Fig. 1c and the surface area S turns out to be

$$S = 2\pi R^2\left(1 - \sqrt{1 - \left(\frac{r}{R}\right)^2}\right) \tag{4}$$

Now, we define the relative curvature, x, by

$$x = \frac{R_0}{R} \tag{5}$$

From Eqs. (2), (3) and (5), we obtain the relationship

$$r = 2R_0\sqrt{1 - x^2} \tag{6}$$

Accordingly, the bending energies, E_{sphere}, and E_{cup}, of the spherical and cup shaped vesicles become

$$E_{\text{sphere}} = \frac{\kappa}{2}\int (c_x + c_y - c_0)^2 \mathrm{d}S = 2\pi\kappa(2 - c_0R_0)^2 \tag{7}$$

$$E_{\text{cup}} = \frac{\kappa}{2}\int (c_x + c_y - c_0)^2 \mathrm{d}S = 2\pi\kappa(2x - c_0 R_0)^2 \tag{8}$$

The bending energy of sheets will be considered in Section 3.

To formulate the theory of the adsorption of talin, we define the total number, X, and the adsorbed number, N, of talin to the orifices of the vesicles in the system volume, V. The partition function Z of the total system is written as

$$Z = Z_{\text{bulk}} Z_{\text{ad}} \tag{9}$$

$$Z_{\text{bulk}} = \frac{1}{(X-N)!}(pf)_{\text{bulk}}^{X-N} \tag{10}$$

$$Z_{ad} = \frac{1}{N!}(pf)_{\text{ad}}^{N}\binom{n_0}{n} \times \exp\left[-\frac{1}{kT}\left(-N\varepsilon_0 + n(E_{\text{cup}} - E_{\text{sphere}})\right)\right] \tag{11}$$

where

$$(pf)_{\text{bulk}} = \lambda^{-3} V \tag{12}$$

$$(pf)_{\text{ad}} = \lambda^{-3}\, 2\pi nrd^2 \tag{13}$$

In Eqs. (10)–(13), the $(pf)_{\text{bulk}}$ and $(pf)_{\text{ad}}$ are the molecular partition functions of a dissolved talin in the aqueous solvent and an adsorbed talin, respectively. Also, n_0, n, and $\binom{n_0}{n}$ in Eq. (11) are the numbers of vesicles and coffee cups and the number of the combinations of choice n from n_0, respectively. In Eq. (11), we denote, ε_0 as an affinity energy of talin from water to the orifice of the vesicle. For computational simplicity, we postulated that the sizes of the spherical vesicles were mono-dispersed in the solution. The factor λ in Eqs. (12) and (13) is the de-Brogrie wave length defined by

$$\lambda = \frac{h}{\sqrt{2\pi mkT}} \tag{14}$$

where h, m, k and T are Planck's constant, mass of a talin molecule, Boltzmann's constant and temperature in Kelvin, respectively. As we are not concerned with the quantum effect (Planck's constant), the resulting physical quantities derived from the partition function will not contain λ at all. In Eq. (13), it is postulated that the adsorbed talin can move around the total volume $2\pi nrd^2$ of the orifices of whole cups. The talin molecule is assumed to be a cube with side d for simplicity.

The free energy, F, of the total system, becomes

$$\begin{aligned} F &= -kT\ln Z \\ &= -(X-N)kt\ln\left(\frac{e\lambda^{-3}V}{X-N}\right) \\ &\quad - NkT\ln\left(\frac{e\lambda^{-3}2\pi nrd^2}{N}\right) - N\varepsilon_0 \\ &\quad + n(E_{\text{cup}} - E_{\text{sphere}}) - kT[n_0 \ln n_0 - n\ln n \\ &\quad - (n_0 - n)\ln(n_0 - n)] \end{aligned} \tag{15}$$

The free energy, F, should be minimized to obtain equilibrium. Here, the term equilibrium refers to the metastable equilibrium in the sense stated in the previous section. Similar formulations and definitions have been used to explain other membrane phenomena by Suezaki [10–12]. The fourth term of the right hand side (RHS) of Eq. (15) is the change of the bending energy from the spherical vesicles to cups. The factor e in Eq. (15) is the root of the natural logarithm.

To minimize the free energy defined above, we take N and n as independent variables. Then, the other variables, x and r are expressed by N and n. The following relationships hold for the defined variables;

$$N = \frac{2\pi nr}{d} \tag{16}$$

$$x = \sqrt{1 - \alpha\left(\frac{N}{n}\right)^2} \tag{17}$$

$$\alpha = \left(\frac{d}{4\pi R_0}\right)^2 \tag{18}$$

By taking the derivatives of F with respect to N and n, we obtain

$$\frac{\partial F}{\partial N} = \mu_{\mathrm{ad}} - \mu_{\mathrm{bulk}} = 0 \tag{19}$$

$$\mu_{\mathrm{bulk}} = kT\ln\left(\frac{X-N}{V}\right) \tag{20}$$

$$\mu_{\mathrm{ad}} = -kT\ln(ed^3) - \varepsilon_0 + 8\pi\kappa n(2x - c_0R_0)\frac{\partial x}{\partial N} \tag{21}$$

$$\frac{\partial F}{\partial n} = E_{\mathrm{cup}} - E_{\mathrm{sphere}} + 8\pi n\kappa(2x - c_0R_0)\frac{\partial x}{\partial n} + kT\ln\left(\frac{n}{n_0 - n}\right) = 0 \tag{22}$$

In Eqs. (20) and (21), the factors μ_{bulk} and μ_{ad} are the chemical potentials of dissolved talin in the aqueous solvent and the adsorbed talin, respectively. From Eq. (17), the following equations are derived.

$$\frac{\partial x}{\partial N} = -\frac{1}{xN}(1 - x^2) \tag{23}$$

$$\frac{\partial x}{\partial n} = \frac{1}{xn}(1 - x^2) \tag{24}$$

From Eqs. (17)–(24), the adsorbed number, N, and x are determined as solutions of the following equations.

$$N = X - \frac{V}{ed^3}\exp\left(-\frac{\varepsilon}{kT}\right) \tag{25}$$

$$\varepsilon = \varepsilon_0 + (2x - c_0R_0)\frac{\kappa d}{xR_0}\sqrt{1 - x^2} \tag{26}$$

$$\frac{1}{8\pi\kappa}\frac{\partial F}{\partial n} = 1 + R_0c_0 - x^2 - \frac{R_0c_0}{x} - \beta\ln\left(\frac{n_0}{n} - 1\right) = 0 \tag{27}$$

$$\beta = \frac{kT}{8\pi\kappa} \tag{28}$$

By using Eqs. (16)–(18), Eqs. (25) and (27) can be solved to obtain N and n as a function of X. Before solving the problem, we will calculate the minimized free energy $F_{\min}$ of the total system. Inserting the result of Eqs. (19)–(22) into Eq. (15), we finally obtain

$$F_{\min} - F_0 = XkT\ln\left(1 - \frac{N}{X}\right) + NkT + n_0kT\ln\left(1 - \frac{n}{n_0}\right) \tag{29}$$

where

$$F_0 = -XkT\ln\left(\frac{e\lambda^{-3}V}{X}\right) \tag{30}$$

is the free energy of a monomer aqueous solution of talin without adsorbing to vesicles. Because the RHS of Eq. (29) is negative, the total free energy is lowered by adsorbing talin to vesicles, rather than the dissolved monomers in the aqueous solution. A further analysis of the above formulation is continued in Section 3.

3. Detailed analysis of the adsorption isotherm of talin to vesicles

In Section 2, we formulated the theoretical algorithm of the adsorption of talin by changing from spherical vesicles to cup-shaped vesicles. In this section, we apply the formula of the previous section to reproduce the observed data of the adsorption of talin to vesicles [3]. Eq. (25) is rewritten as

$$C_N = C_X - C_{th} \tag{31}$$

where

$$C_N = \frac{N}{V} \tag{32}$$

$$C_X = \frac{X}{V} \tag{33}$$

are the adsorbed and total concentrations of talin, respectively, and

$$C_{th} = \frac{1}{ed^3}e\left(-\frac{\varepsilon}{kT}\right) \tag{34}$$

is the threshold concentration for the adsorption of talin. Although we cannot address the exact value of C_{th}, the value is estimated to be around 1 μM according to the observed data [3]. Because the second term of Eq. (26) is small compared with the first term, we approximately estimate the value of ε_0 as follows

$$\varepsilon_0 = 20.2\,kT \tag{35}$$

from Eq. (34), where we assumed $d = 10$ nm. If we consider the large molecular weight of talin, the value of Eq. (35) may be reasonable.

Next, the number, n_0, of the initial spherical vesicles is determined by the relationship

$$\frac{N_L}{n_0} = \frac{8\pi R_0^2}{s} \tag{36}$$

where the factors, N_L and s are the total number of lipid molecules and the occupied surface area per lipid molecule on the membrane, respectively. By using the various factors defined previously, the ratio n_0/n in Eq. (27) becomes

$$\frac{n_0}{n} = \frac{s}{2dR_0}\frac{C_L}{(C_X - C_{th})}\sqrt{1-x^2} \tag{37}$$

where C_L is the concentration of lipid defined by

$$C_L = \frac{N_L}{V} \tag{38}$$

Eq. (27) is rewritten in the following form

$$1 + R_0c_0 - x^2 - \frac{R_0c_0}{x} = \beta\ln\left(\frac{n_0}{n} - 1\right) \tag{39}$$

From Eqs. (37) and (39), the relative curvature x is determined as a function of the concentration C_X of talin. Examples of the left-hand side (LHS) of Eq. (39) are plotted in Fig. 2 for several values of R_0c_0.

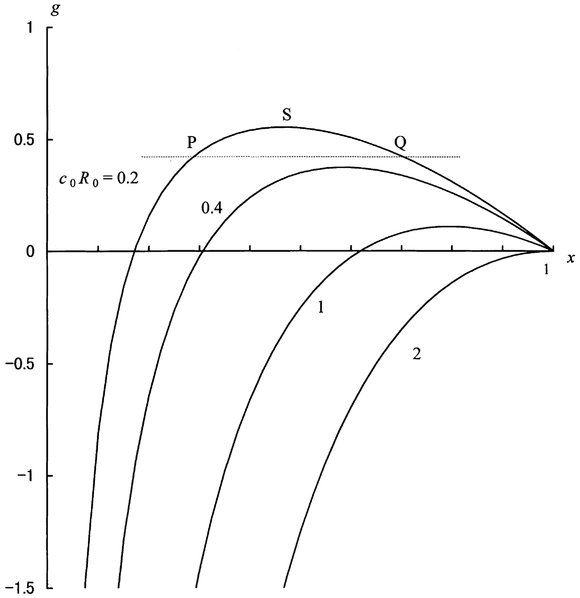

Fig. 2. The change of Eq. (39) as a function of x for several values of R_0c_0.

Because the factor, β in Eq. (39) is small compared with unity, the effect of $\sqrt{1-x^2}$ in Eq. (37) for determining x can be neglected as a first approximation. Although there exists two solutions of x, as can be seen in Fig. 2 for an appropriate concentration, the smaller solution of x shown as the point P is the correct one. The other, point Q, is not correct, and corresponds to the free energy maximum point. By solving Eqs. (37) and (39), x decreases and the number n of cups increases, when the concentration C_X increases. This fact is consistent with the observed data. Also, it is expected that the orifice with finite size appears after reaching another threshold concentration larger than C_{th} as shown in Fig. 2 as point S. The typical shape seen in the data [3] corresponds to approximately $x \leq 0.8$. The curve for $c_0R_0 = 1$ in Fig. 2 corresponds to this case. In this case, we can say that the radius of the spontaneous curvature of spherical vesicles is expected to be $R_0 = 1/c_0$. In many other cases, the radius of the orifice of coffee cups becomes larger from a small size by increasing the concentration of talin [3]. This fact shows that the point S in Fig. 2 corresponds to $x = 1$ and $R_0 = 2/c_0$. The initial spherical vesicles without frustration generate coffee cups with small orifices at the threshold concentration of talin. On the other hand, the vesicles with negative spontaneous curvatures may remain spherical, because Eq. (39)

does not have a solution for x to form coffee cups.

We now assume that the spontaneous curvature is zero in Eq. (39). Then, the LHS becomes a monotonous decreasing function of x. In this case, we can not obtain a solution that minimizes the free energy. Thus, positive spontaneous curvatures of the vesicle is the necessary condition to form a cup shaped vesicle. If there are spherical vesicles with negative spontaneous curvatures, they can not be candidates for cup-shaped vesicles.

Before moving on to the next topic, we will discuss the minimized energy $F_{\min}$ in Eq. (29). As the last term of the RHS of Eq. (29) is small compared with the other terms, we will neglect the last term for further analysis. Then, the minimized free energy, f, per molecule scaled by kT becomes

$$f = \frac{F_{\min} - F_0}{XkT} = 1 - \frac{C_{th}}{C_X} - \ln\left(\frac{C_X}{C_{th}}\right) \tag{40}$$

by using the definitions of Eqs. (33) and (34). If we neglect the small correction of C_{th} as a function of C_X, the change of f as a function of C_X/C_{th} is shown in Fig. 3. The important point is that the function, f, possesses an inflection point at $C_X = 2C_{th}$, as schematically shown in Fig. 3. The meaning of this fact will be discussed in the following paragraphs.

Next, we will discuss the possibility of the coexistence of coffee cups and sheet-shaped vesicles observed in the experimental report [3]. Even though the observed sheet shaped vesicles seem to possess small curvatures, the sheet shaped vesicles are modeled as a flat elliptic sheet, as schematically drawn in Fig. 4. We defined the lengths a and b as shown in Fig. 4. The eccentricity, e, of the ellipse, by definition, becomes

$$e = \sqrt{\frac{a^2 - b^2}{a^2}} \tag{41}$$

The area of the ellipse is πab, and the length of the periphery L is expressed from the formula of elliptic function (second class) as

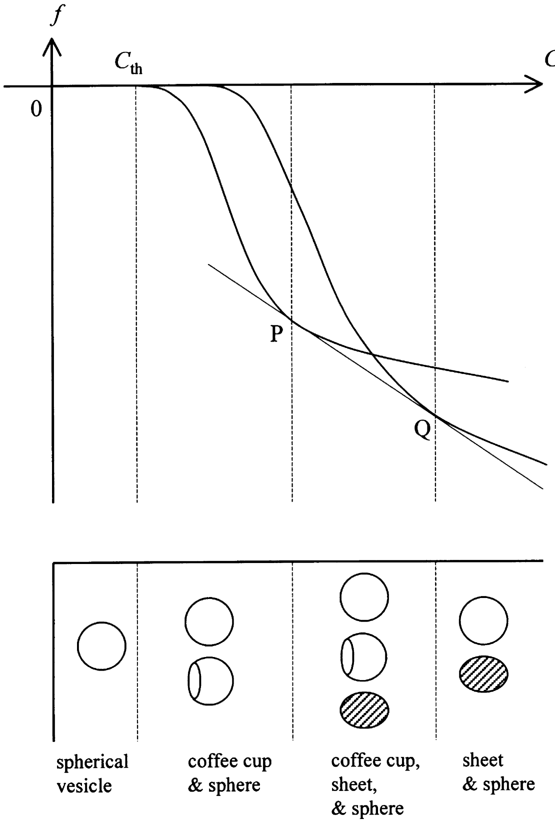

Fig. 3. Schematic drawing of the minimized free energy, f [Eq. (40)] as a function of the concentration C_X of talin. The curves A and B are for coffee cup and ellipse. The lower part is the schematic drawing of the phase diagram.

$$L = 4\pi R_0 g(e) \tag{42}$$

where

$$g(e) = \frac{1}{(1-e^2)^{1/4}} \frac{1}{1+\delta}\left(1 + \frac{\delta^2}{2} + \frac{\delta^4}{64} + \dots\right) \tag{43}$$

$$\delta = \frac{1 - \sqrt{1-e^2}}{1 + \sqrt{1+e^2}} \tag{44}$$

The corresponding equations to Eqs. (26) and (27) become

$$\varepsilon = \varepsilon_0 \tag{45}$$

$$\frac{1}{8\pi\kappa}\frac{\partial F}{\partial n}=R_0c_0-1-\beta\ln\left(\frac{n_0}{n}-1\right)=0 \tag{46}$$

The profile of the free energy f per molecule is also shown in Fig. 3 with a slightly different value of C_{th}. In this case, however, C_{th} is constant, different from that of the coffee cup. Eq. (46) is rewritten as

$$n=\frac{n_0}{e^{\frac{\Delta E}{kT}}+1} \tag{47}$$

where $\Delta E=8\pi\kappa(c_0R_0-1)$. According to the observed data [3], almost all spherical vesicles are converted to sheet like vesicles, so that n in Eq. (47) is expected to be close to n_0. In other words, ΔE in Eq. (47) is expected to be negative. By a similar procedure shown before, the relationship corresponding to Eq. (16) becomes

$$\frac{N}{n}=\frac{L}{d}=\frac{4\pi R_0}{d}g(e) \tag{48}$$

Finally, we obtain the equation which determines the eccentricity, e, as follows;

$$g(e)=\left[1+\exp\left(\frac{\Delta E}{kT}\right)\right]\frac{2R_0d}{s}\frac{C_X-C_{th}}{C_L} \tag{49}$$

The above equation shows that the eccentricity of the ellipse can be evaluated directly as a function of C_X. By increasing the concentration C_X, the circle with the radius $2R_0$ appears at $e=0$. After the formation of a circle, it deforms to an ellipse as the value of C_X increases. Even though the free energy profile f of Eq. (40) is formally identical to the cup-shaped vesicle, however, the C_{th} in Eq. (49) is a constant different from that of the coffee cup vesicles. In the case of the coffee cup vesicle, the effective affinity energy ε changes as a function of the concentration C_X through Eqs. (39) and (26). From this difference of the concentration dependence of the affinity energy ε, the two energy profiles possess the common tangent P to Q, as shown schematically in Fig. 3. The expected shape change of the vesicles based on the above energy profiles is also shown in Fig. 3. The actual vesicles observed are not an ellipsis but sheets that possess a more complex periphery. The elliptic shape is a model for mathematical simplicity and clarity of the evaluation. The function $g(e)$ is calculated and shown in Fig. 5. The cross section of the curve and the horizontal line determines the eccentricity, e, as a function of the concentration of talin, C_X. The possibilities of flat vesicles with rectangular shape were also analyzed. However, the concentration range of the rectangle was shown to be higher than that of the ellipse.

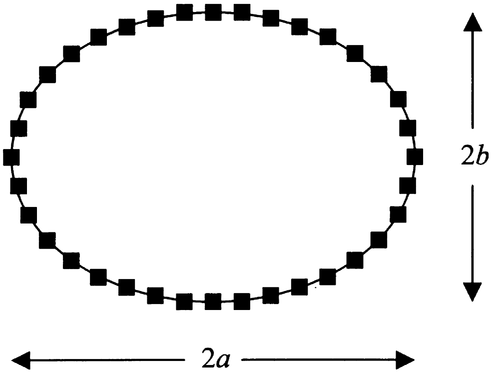

Fig. 4. Schematic picture of a elliptic sheet vesicle.

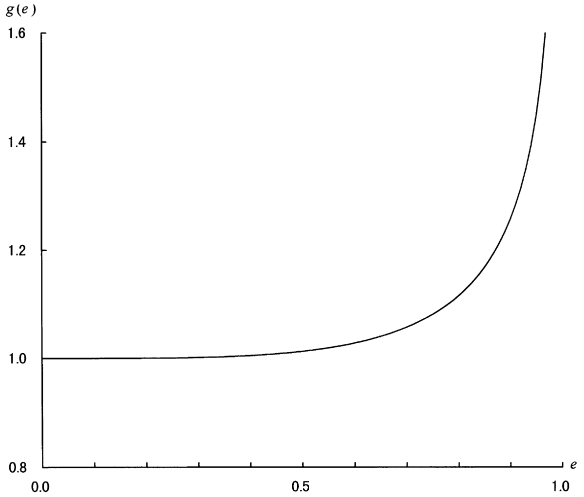

Fig. 5. The factor $g(e)$ as a function of eccentricity, e.

Although rare, deformed spheres with two orifices were observed in the experiment [3]. The schematic picture of this vesicle is shown in Fig. 6. We will analyze the possibility of this vesicle by a procedure similar to the one given above. The surface area S of this vesicle becomes

$$S = 4\pi R^2 \sqrt{1 - \left(\frac{r}{R}\right)^2} \tag{50}$$

From Eqs. (3) and (5), we obtain

$$r = \frac{R_0}{x}\sqrt{1 - x^4} \tag{51}$$

The number of adsorbed talin molecules per vesicle becomes

$$N = \frac{4\pi n r}{b} \tag{52}$$

Although we do not show the detailed procedure of this calculation, the equation that corresponds to Eq. (39) becomes

$$\begin{aligned} x^2 - c_0 R_0 x + c_0 R_0 - 1 + x(2x - c_0 R_0)\frac{1 - x^4}{1 + x^4} \\ = \beta \ln\left(\frac{n_0}{n} - 1\right) \end{aligned} \tag{53}$$

The affinity energy ε turns out to be

$$\varepsilon = \varepsilon_0 - \frac{2b\kappa}{R_0}(2x - c_0 R_0)x^2 \frac{\sqrt{1 - x^4}}{1 + x^4} \tag{54}$$

Although we do not show it here, the left-hand side of Eq. (53) for several values of c_0 has been calculated. The maximum values of these as functions of x are lower than those of Eq. (39) for the same c_0. This means that the vesicles with two orifices should appear in a higher concentration range than that of coffee cups. The experimental data are consistent with this fact. Different from the case of cups, the LHS of Eq. (53) behaves as an increasing function of x, even when the spontaneous curvature is zero.

The coexistence of the cups and vesicles with two orifices with different spontaneous curvature can also be considered and could be analyzed. However, we will not proceed further with the calculation. This is because the observed data [3] are not precise enough to quantitatively evaluate the theoretical parameters introduced in this theory.

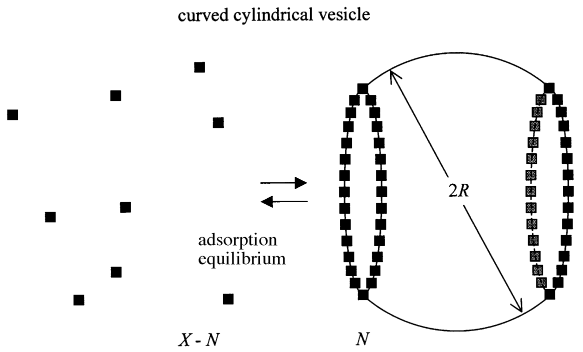

Fig. 6. Schematic picture of the partial sphere with two orifices.

4. Conclusion and discussion

The adsorption of protein molecule (talin) to the orifice of coffee cup shaped vesicles, deformed from spherical lipid vesicles, was analyzed by the statistical mechanical theory. The bending energy of the membrane was taken as the mechanical energy of the vesicle deformation. By minimizing the free energy of the total system of talin and lipid, the adsorbed number of talin molecules and the shape of the cup were determined as functions of the concentration of talin. The expected concentration dependence was qualitatively consistent with the observed experimental data. The vesicle with an elliptical shape was also analyzed and was shown to coexist with the cup shaped vesicle.

A positive spontaneous curvature for the bilayer membrane was shown to be the necessary condition for the formation of the coffee cup vesicles. The observed shapes of the cups are not exactly partial spheres cut by a plane, but rather elongated spheres from the orifice. Although not shown in this report, the assumption of spheroids cut by a plane could lower the energy more than that of the partial spheres. Additionally, some line torque from the inside cup to the outside cup may work along the orifice. At this point, a more detailed analysis is required.

The vesicle is an open system due to the adsorption of talin between the aqueous solution and the periphery of the vesicles. Therefore, a comprehensive understanding of the mechanical force balance is not easily obtained. Thus, we will estimate the line tension energy of a coffee cup vesicle. From Eq. (8), we can describe the mechanical energy of a coffee cup vesicle as

$$E_{\mathrm{cup}} = 2\pi\kappa(2x - c_0 R_0)^2 + 2\pi r \varepsilon_L \quad (55)$$

where ε_L is the apparent line tension energy per unit length of the orifice. Using Eqs. (5) and (6), the mechanical balance of the vesicle is described as

$$\frac{\mathrm{d}E_{\mathrm{cup}}}{\mathrm{d}r} = -\frac{4\pi\kappa r}{xR_0^2}(2x - c_0 R_0) + 2\pi\varepsilon_L = 0 \quad (56)$$

Then, the line tension energy, ε_L, becomes

$$\varepsilon_L = \frac{2\kappa r}{xR_0^2}(2x - c_0 R_0) \quad (57)$$

The line tension is positive when the spontaneous curvature is not large in the early stage of cup formation ($x = c_0 R_0/2$). Its absolute value is an increasing function of r when the radius r is small. The order of the magnitude of the line tension per molecule is roughly $\kappa d/R_0$, which is small compared with kT. The idea of line tension has already been introduced by others [13–15].

Although we postulated a monodispersed vesicle solution with the same spontaneous curvature throughout the analysis, a polydispersity with respect to the size of the vesicles and the difference of the spontaneous curvature might exist in the observed system. The extension of our theory to the polydispersity of vesicles is a problem for future studies. Lastly, the real-time dynamics of the beginning of cup formation will be one of the challenges for future work.

Acknowledgements

This work was partly supported by the Ministry of Education, Science, Sports, and Culture of Japan (grant No. 10640372). We thank Dr Lisa Filippi for her assistance in preparing the manuscript.

References

[1] T. Kaneko, T.J. Itoh, H. Hotani, J. Mol. Biol. 284 (5) (1998) 1671.
[2] M. Honda, K. Takiguchi, S. Ishikawa, H. Hotani, J. Mol. Biol. (1999) in press.
[3] A. Saitoh, K. Takiguchi, Y. Tanaka, H. Hotani, Proc. Natl. Acad. Sci. USA 95 (1998) 1026.
[4] W. Helfrich, Z. Naturforsch. 28c (1973) 693.
[5] T. Sekimura, H. Hotani, J. Theor. Biol. 149 (1990) 325.
[6] T. Umeda, H. Nakajima, H. Hotani, J. Phys. Soc. Jpn. 67 (1998) 682.
[7] W. Helfrich, Z. Naturforsch. 29c (1974) 510.
[8] H.J. Deuling, W. Helfrich, Blood Cells 3 (1977) 713.
[9] Y. Suezaki, Biophys. Chem. 65 (1997) 101.
[10] Y. Suezaki, J. Theor. Biol. 71 (1978) 279.
[11] Y. Suezaki, J. Colloid Interface Sci. 73 (1980) 529.
[12] Y. Suezaki, J. Dispersion Sci. Tech. 4 (1983) 371.
[13] W. Helfrich, Phys. Lett. 50A (1974) 115.
[14] R. Lipowsky, J. Phys. France II 2 (1992) 1825.
[15] R. Lipowsky, Biophys. J. 64 (1993) 1133.